Am J Physiol Heart Circ Physiol 293: H557–H562, 2007.
First published March 30, 2007; doi:10.1152/ajpheart.01095.2006.

Reduced systolic wave generation and increased peripheral wave reflection in chronic heart failure

Stephanie L. Curtis,[1] Andrew Zambanini,[1] Jamil Mayet,[1] Simon A. McG Thom,[1] Rodney Foale,[1] Kim H. Parker,[2] and Alun D. Hughes[1]

[1]*International Centre for Circulatory Health, and* [2]*Department of Bioengineering, Faculty of Engineering, Saint Mary's Hospital and Imperial College, London, United Kingdom*

Submitted 6 October 2006; accepted in final form 23 March 2007

Curtis SL, Zambanini A, Mayet J, McG Thom SA, Foale R, Parker KH, Hughes AD. Reduced systolic wave generation and increased peripheral wave reflection in chronic heart failure. *Am J Physiol Heart Circ Physiol* 293: H557–H562, 2007. First published March 30, 2007; doi:10.1152/ajpheart.01095.2006.—In human heart failure the role of wave generation by the ventricle and wave reflection by the vasculature is contentious. The aim of this study was to compare wave generation and reflection in normal subjects with patients with stable compensated heart failure. Twenty-nine normal subjects and 67 patients with heart failure (New York Heart Association class II or III) were studied by noninvasive techniques applied to the common carotid artery. Data were analyzed by wave intensity analysis to determine the nature and direction of waves during the cardiac cycle. The energy carried by an early systolic forward compression wave (S wave) generated by the left ventricle and responsible for acceleration of flow in systole was significantly reduced in subjects with heart failure ($P < 0.001$), and the timing of the peak of this wave was delayed. In contrast, reflection of this wave was increased in subjects with heart failure ($P < 0.001$), but the timing of reflections with respect to the S wave was unchanged. The energy of an expansion wave generated by the heart in protodiastole was unaffected by heart failure. The carotid artery wave speed and the augmentation index did not significantly differ between subjects with heart failure compared with normal individuals. The ability of the left ventricle to generate a forward compression wave is markedly impaired in heart failure. Increased wave reflection serves to maintain systolic blood pressure but also places an additional load on cardiac function in heart failure.

cardiac function; blood pressure

THE PUMP FUNCTION OF THE HEART depends on its interaction with the vasculature. Many methods of evaluating cardiac function rely either solely on assessment of the heart or focus on pressure changes occurring in the vasculature. However, an examination of either aspect of cardiac function in isolation does not give an adequate insight to the dynamic interaction between the two. In heart failure this interaction remains poorly characterized but may have important implications for optimization of therapy (2). Analysis of the end-systolic pressure-volume relationship and the ratio of end-systolic pressure to stroke volume [effective arterial elastance] has been used to assess arterioventricular coupling (29), but the measurement of end-systolic pressure-volume relationship and arterial elastance in heart failure generally involves invasive measurements, and the technique has not yet found widespread use in the clinical assessment of heart failure.

It has been proposed that, in heart failure, alterations in wave reflection contribute to impaired cardiac output (20, 21). Studies examining impedance changes in heart failure have yielded conflicting results (4, 13, 15, 17, 18, 25), but it has been suggested that wave speed is increased in heart failure [possibly as a consequence of peripheral vasoconstriction and endothelial dysfunction (26)] and that, as a result, reflected waves normally present in diastole return in systole, increasing left ventricular wall stress and attenuating ejection (20, 21). Despite its potential importance, this hypothesis remains unconfirmed.

Wave intensity analysis is a new technique that analyzes vascular hemodynamics in terms of traveling energy waves. These waves can be calculated at any point in the circulation if local pressure and flow changes are known (23). From these measurements this analysis can calculate the intensity of the wave (i.e., its power per unit cross-sectional area), the absolute energy carried per unit cross-sectional area by a wave, the direction of wave travel, and the wave type (i.e., whether it will accelerate or decelerate flow). In addition, this approach can be used to separate forward and backward (reflected) waves contributing to the pressure waveform and to quantify local wave speed, a measure of arterial stiffness. This technique was initially used with invasive measurements of pressure and flow (23) and more recently using ultrasound-based techniques alone (22) or in conjunction with applanation tonometry (32). In this study we have used the latter noninvasive approach to measure wave intensity in humans. The aims of this study were to investigate the effect of heart failure on cardiac generation of waves and to establish whether wave reflection, wave speed, or wave timing are altered in heart failure.

METHODS

Study population. The study was approved by the St. Mary's Hospital Local Research Ethics Committee, and all subjects gave informed consent. Twenty-nine normal subjects (13 men; ages, 40–79 yr) who had no history of cardiac disease or hypertension and were receiving no medication were compared with 67 patients with compensated systolic heart failure [New York Heart association (NYHA) class II or III], treated with diuretics and an angiotensin-converting enzyme inhibitor (or angiotensin receptor blocker). Patients with heart failure were recruited from the Peart Rose Cardiovascular Disease

Address for reprint requests and other correspondence: A. D. Hughes, Clinical Pharmacology, National Heart and Lung Div., Faculty of Medicine, Imperial College London, QEQM Wing, St. Mary's Hospital, S. Wharf Rd., London W2 1NY, UK (e-mail: a.hughes@imperial.ac.uk).

The costs of publication of this article were defrayed in part by the payment of page charges. The article must therefore be hereby marked "*advertisement*" in accordance with 18 U.S.C. Section 1734 solely to indicate this fact.

Table 1. *Baseline characteristics of heart failure patients and normal subjects used in the comparative study*

	Normal	Heart Failure	*P* Value
n	29	67	
Age, yr	60 (SD 9)	66±(SD 10)	0.004
Men (%)	13 (45)	42 (63)	0.1
SBP, mmHg	124 (SD 18)	126 (SD 25)	0.6
DBP, mmHg	75 (SD 9)	70 (SD 11)	0.07
PP, mmHg	47 (SD 15)	58 (SD 18)	0.07
cSBP, mmHg	116 (SD 4)	115 (SD 3)	0.2
Peak *U*, m/s	0.70 (SD 0.15)	0.57 (SD 0.16)	<0.001
Heart rate, beats/min	67 (SD 9)	71 (SD 14)	0.2
Height, m	1.69 (SD 0.11)	1.65 (SD 0.10)	0.1
Weight, kg	73.8 (SD 12.7)	74.4 (SD 16.2)	0.9
BMI, kg/m^2	25.9 (SD 3.4)	27.2 (SD 5.0)	0.2
NYHA, class II/III (%)	ND	40 (60)/27 (40)	—
Left ventricular internal diastolic diameter, cm	ND	5.8 (SD 1.1)	—
Left ventricular mass, g	ND	362 (SD 126)	—
Cardiac output, l/min	ND	2.3 (SD 1.0)	—
Ejection fraction, %	ND	39 (SD 18)	—

Data are means (SD); *n*, number of subjects. SBP, systolic blood pressure; DBP, diastolic blood pressure; PP, pulse pressure; cSBP, carotid systolic blood pressure; peak *U*, peak carotid flow velocity; BMI, body mass index; NYHA, New York Heart Association; ND, no data.

Prevention Clinic, St Mary's Hospital, and normal subjects were recruited by advertisement among the staff of Imperial College (London, UK).

Measurement of carotid pressure and flow waveforms. A detailed description of the methodology and reproducibility of the techniques used in this study has been published recently (32, 33). All experiments were performed in a quiet, darkened room at a temperature of 25°C, and all subjects refrained from smoking, alcohol, and caffeine consumption for 24 h before the study. Supine brachial blood pressure was measured as the average of the last two of three measurements made in the left arm after 10 min of rest using a semiautomated, validated oscillometric blood pressure monitor (Omron HEM-705CP).

Measurements of carotid arterial blood pressure were made at the right common carotid artery using a high-fidelity strain-gauge arterial tonometer (SPT-301, Millar Instruments, Houston, Tx) (1), and mean and diastolic pressures were calibrated to brachial artery measurements as previously described (9). This technique has been shown to be valid (9, 31) and reproducible (28, 33). Pressure waveforms and simultaneous ECG traces were acquired for 15–20 cardiac cycles, and data were digitized at 200 Hz. Flow velocity measurements were made in a 1.5-mm Doppler sample volume located in the center of the arterial lumen, ~2 cm from the carotid bulb using pulsed-wave Doppler with an HDI 5000 ultrasound machine (Philips Medical Systems, Best, The Netherlands) and a 7.5- to 10-MHz linear array transducer at a fixed Doppler angle of 60° to minimize error in velocity estimates (5). ECG was acquired concurrently, and ~20 cardiac cycles were recorded and digitized at 200 Hz. Doppler data were analyzed using commercially available software (HDI, Philips Medical Systems) and custom-written software in Matlab 5.3 (The Mathworks). Pressure and flow waveforms (4–6 waveforms) were ensemble averaged using the ECG R wave as an indicative fiducial marker, i.e., the initial alignment of pressure and flow was undertaken using this marker. Subsequently, an alignment of the ensembled pressure and flow waves was checked visually and, if necessary, adjusted to ensure no temporal misalignment before analysis. Carotid artery wave speed was calculated using a pressure-flow velocity loop as previously described (11, 32). From the conservation of mass and momentum, there is a simple relationship between the changes in pressure and flow velocity that is valid when only a forward-traveling wave is present; this relationship is given by the "waterhammer" equation: $dP_{\pm} = \rho c dU_{\pm}$ (*Eq. 1*), where dP is the measured change in pressure (P), d*U* is the measured change in flow velocity (*U*) over one sampling period, + is forward and − is backward, ± is forward and backward, ρ is the density of blood (1.06 g/cm^3), and *c* is the local wave speed. If the ensemble-averaged pressure and velocity data are plotted, there is a linear portion of the loop corresponding to the earliest part (50 ms) of arterial systole (see Ref. 32, for example). This indicates that during this time there are no reflected waves present. During this early period of arterial systole, *c* is equal to the gradient of the line describing the relationship between pressure and flow velocity, and, using *Eq. 1*, local wave speed can be calculated.

Forward and backward waves and the components of the measured change in pressure and flow velocity were determined from the following equations derived from the method of characteristics (23, 32): change in pressure, $dP_{\pm} = 1/2(dP \pm \rho c dU)$ (*Eq. 2*); and change in flow velocity, $dP_{\pm} = 1/2(dU \pm dP/\rho c)$ (*Eq. 3*).

The forward- and backward-pressure waveforms were determined by an integration of the forward- and backward-traveling changes in pressure, and, from these, maximum forward and backward pressure could be calculated. An integration constant was included arbitrarily in the forward pressure and was taken to be the minimum value of P. The integration constant for *U* was zero.

Forward and backward wave intensities (*I*) were calculated as follows: $dI_{\pm} = dP_{\pm}dU_{\pm}$ (*Eq. 4*).

Forward wave intensities had a magnitude greater than zero, whereas backward wave intensities had a magnitude less than zero.

Compression waves were defined as occurring during positive changes in pressure and expansion waves during negative changes. The time of onset and offset of each wave was determined manually using electronic crosshairs, and the error in timings was <5 ms. Wave energy was determined by integrating the area under the wave-intensity curve between these two time points. The time of onset of each wave was determined relative to the onset of the first forward compression wave (S). The time of onset of the S wave relative to the fiducial ECG R wave was also determined (32). Augmentation index (AI_x), the pressure difference between the "shoulder" of the carotid artery pressure waveform and the peak carotid systolic pressure expressed as a percentage of the pulse pressure, was calculated as described by Kelly et al. (10).

Table 2. *Comparison of normal subjects and heart failure patients*

	Normal	Heart Failure	*P* Value
n	29	67	
S wave energy, mJ/m^2	745±46	467±29	<0.001
Time of peak S wave, s	0.12±0.01	0.15±0.01	0.001
R wave energy, mJ/m^2	75±13	73±8	0.9
Time of peak R wave, s	0.19±0.01	0.22±0.01	0.025
S to R wave interval, s	0.07±0.01	0.07±0.01	0.6
X wave energy, mJ/m^2	34±6	6±4	<0.001
Time of peak X wave, s	0.21±0.01	0.24±0.01	0.033
S to X wave interval, s	0.08±0.01	0.09±0.01	0.9
D wave energy, mJ/m^2	149±16	144±11	0.8
Time of peak D wave, s	0.39±0.05	0.37±.05	0.13
S to D wave interval, s	0.26±0.01	0.22±0.01	<0.001
Total reflection, %	13.8±3.7	24.9±2.3	0.015
Body reflection, %	1.5±1.0	5.0±0.7	0.006
Head reflection, %	12.3±3.2	19.9±2.0	0.06
Peak flow velocity, m/s	0.71±0.03	0.57±0.20	0.001
Time of peak velocity, s	0.17±0.01	0.20±0.01	0.003
Carotid artery wave speed, m/s	14.2±1.4	14.0±0.9	0.9
Augmentation index, %	19.3±2.7	24.6±1.7	0.1

Data are means ± SE adjusted for age and sex; *n*, number of subjects. All timings are with respect to the peak R wave. *P* values were calculated by analysis of variance.

Echocardiography was performed in all subjects with heart failure using an ATL HDI 5000 ultrasound machine and a 2- to 4-MHz linear array probe. Left ventricular measurements were made in accordance with the American Society of Echocardiography guidelines using M-mode and Doppler (27). Ejection fraction was calculated by Simpson's rule wherever possible (48 of 67 patients). If good apical views were not obtained, ejection fraction was calculated from two-dimensional parasternal measurements.

Statistical analysis. Data are presented as means (SD) or means ± SE as specified. Unpaired Student's *t*-tests (2-tailed) or ANOVA were used to compare groups. Statistical analyses were performed using an Intercooled Stata 8.2 for Windows (Stata). Statistical significance was assumed if $P < 0.05$.

RESULTS

Subjects with heart failure were older than normal subjects, but, in other respects, groups were well matched (Table 1). Brachial systolic and diastolic pressure and carotid systolic pressure did not differ between groups (Table 1), but peak flow velocity in the carotid artery was significantly reduced in subjects with heart failure compared with normal subjects, and the time in the cardiac cycle when peak flow occurred was also delayed (Table 2).

Wave patterns in heart failure compared with normal subjects. The separated pressure and flow waveforms and the pattern of wave intensities in the common carotid artery of a normal subject and of a patient with heart failure are compared in Figs. 1 and 2. Brachial and carotid blood pressure did not differ between normal subjects and those with heart failure, but peak flow velocity was significantly reduced in heart failure (Table 2). Heart failure was associated with a marked reduction in the energy carried by the S wave, reduced peak S-wave intensity, and a delay in the time of the peak of the S wave (Table 2). Further analysis showed that the reduced S-wave energy in heart failure was unaffected by multivariate adjustment for systolic or diastolic blood pressure, sex, heart rate, or body mass index (BMI) or a combination of all these factors. S-wave energy was progressively reduced with increasing NYHA class [normals = 741 mJ/m^2 (SD 32), NYHA II = 513 mJ/m^2 (SD 24), NYHA III = 399 mJ/m^2 (SD 36); $P < 0.001$ by ANOVA] but did not correlate with LV mass (adjusted $r^2 = 0.06$; $P = 0.2$, adjusted for age and sex), ejection fraction (adjusted $r^2 = 0.03$; $P = 0.8$, adjusted for age and sex), transmitral E wave (adjusted $r^2 = 0.08$; $P = 0.8$, adjusted for age and sex), transmitral A wave (adjusted $r^2 = 0.13$; $P = 0.08$, adjusted for age and sex), or E-to-A ratio (adjusted $r^2 = 0.09$; $P = 0.3$, adjusted for age and sex) in subjects with heart failure.

Although the S-wave energy was reduced in heart failure, the total wave energy reflected was similar between normal and

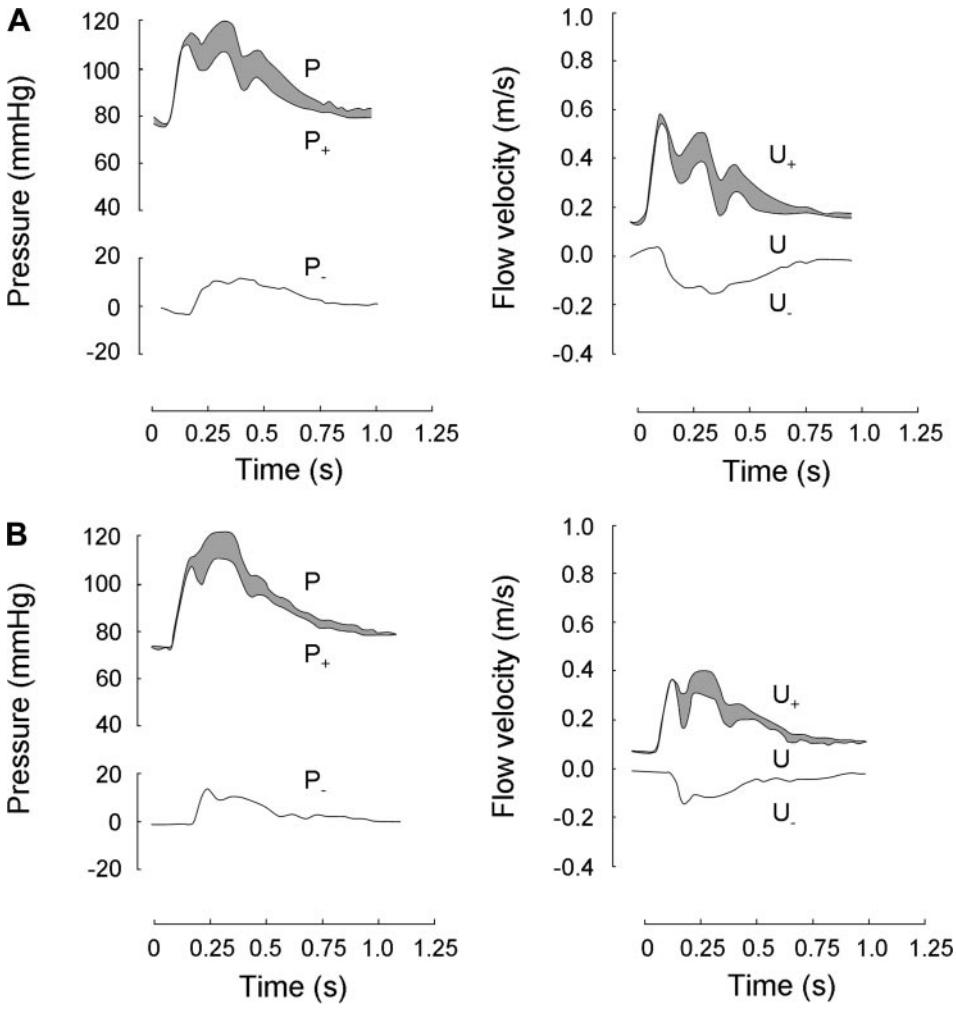

Fig. 1. Total, forward, and backward pressure and flow waveforms in the common carotid artery in a representative normal male subject (age, 55 yr; *A*) compared with a male subject with heart failure (age, 56 yr; *B*). Measured total pressure (P) and flow velocity (*U*) have been separated into forward and backward components using wave intensity analysis. Backward pressure (P_-) adds to forward pressure (P_+) to augment total pressure (P) (the difference between the forward and total pressure waveform, i.e., backward-reflected pressure, is highlighted in gray). In contrast, in the case of flow, backward flow (U_-) decreases forward flow (U_+) so the forward component of flow exceeds total (measured) flow (*U*).

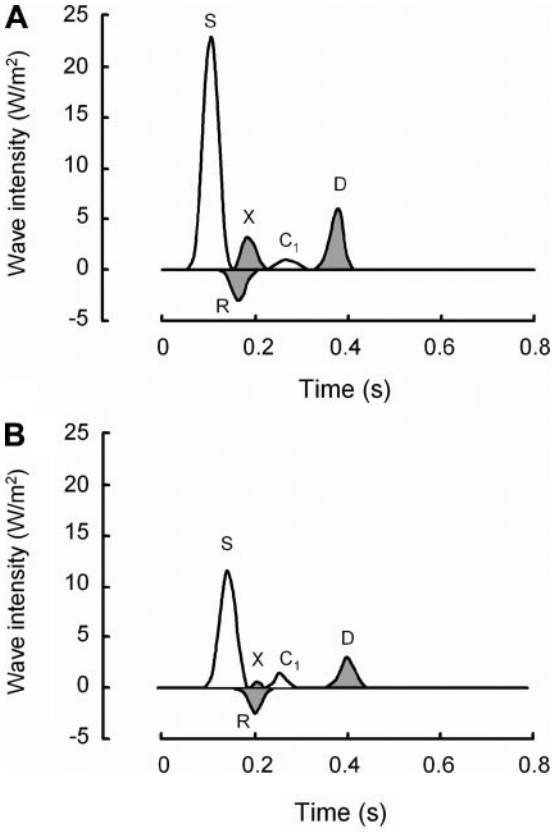

Fig. 2. Wave intensity pattern measured in the common carotid artery in a representative normal male subject (age, 55 yr; *A*) compared with a male subject with heart failure (age, 56 yr; *B*). The characteristic peaks (S, R, X, C_1, and D) are present in both cases. Forward-traveling waves are shown above the zero line, and backward-traveling waves are shown below. Waves that accelerate flow are unshaded, whereas those that decelerate flow are shaded gray. The magnitude of S is reduced markedly in heart failure, and its timing is delayed. The reflected wave from the body (C_1), though small, is increased, especially in proportion to the incident S wave. Traces are taken from the same subjects as in Fig. 1.

heart failure subjects. Consequently, reflection expressed as a percentage of the incident S wave was increased markedly in heart failure (Table 2). Reflected waves in the carotid artery arise from sites of impedance mismatching in the head and body; these reflected wave are associated with a rise in pressure and a decrease in flow. Reflections from the head are seen as a backward-traveling wave (R; Fig. 2) in the carotid artery, whereas reflections from the body will be seen as a forward-traveling wave (C1; Fig. 2). Heart failure was associated with a significant increase in the forward-traveling wave (C1; Fig. 2) that is attributed to reflection from the body. The energy reflected from the head was also increased, but this was of borderline statistical significance. The timing of reflected waves was unaltered by heart failure, but the magnitude of the midsystolic rereflected expansion (X) wave was significantly reduced.

The energy of the D wave was not affected by heart failure, but the interval between the S and D waves (which approximates to ejection time) was significantly reduced in heart failure (Table 2). Carotid artery wave speed and AI_x did not differ significantly between groups (Table 2).

DISCUSSION

We have used wave intensity analysis to compare cardiac wave generation and arterial wave reflection in a large group of normal subjects and subjects with compensated heart failure. We have shown that heart failure is associated with reduced flow velocity in the carotid artery, a marked reduction in wave energy generated by the heart in systole, and increased magnitude of wave reflection from the periphery. The increased reflection may serve to maintain blood pressure at the expense of reduced flow velocity, resulting in an increased load on the left ventricle (20, 21).

Previous studies of wave reflection in heart failure have employed frequency-based impedance techniques using data obtained invasively (4, 14, 15, 17, 25). These studies have yielded conflicting results, possibly due to their small size and the difficulty of obtaining unequivocally normal subjects eligible to undergo invasive measurements of pressure and flow. Wave intensity analysis yields novel hemodynamic information about the heart and its interaction with the vasculature. The interpretation of these data is simplified since they are presented in the time domain and permits the direction, timing, and effect of waves to be determined.

As previously described (6, 23, 32), the normal pattern of waves consisted of a large initial forward-traveling wave (S wave) that accelerates flow. This wave is due to systolic ventricular contraction (6, 23), and the peak of this wave occurred ~130 ms after the ECG R wave. This was followed ~70 ms later by a reflected wave (R wave) arising from the head and neck. Approximately 20 ms later, there was a forward-traveling expansion wave (X) of slightly smaller magnitude than R, which, in the carotid artery, is thought to be a re-reflection of the R wave (32) at a site of impedance mismatching (in the backward direction) at the origin of the common carotid artery from the brachiocephalic artery (a bifurcation that is well matched in the forward direction must inevitably be ill matched in the backward direction). This impedance mismatch will give rise to a reflection of an "open end" type (expansion wave) since the sum of the cross-sectional areas of the brachiocephalic and subclavian arteries is greater than that of the common carotid artery. A later reflected compression wave (C_1) was seen ~150 ms after the initial S wave. The origin of this wave in the carotid artery remains to be established definitively, but we attribute it to reflections that travel in a retrograde manner via the aorta into the carotid artery; hence, it is seen as a forward-traveling compression wave that accelerates flow. Observations in the human aorta (12) have previously identified a reflected wave of similar magnitude and timing in the aorta that corresponds closely with the appearance of this wave in the carotid artery, and reflections traveling via the aorta are likely to be seen after those from the head since they have further to travel. Finally, a large forward-traveling expansion wave (D) was seen at the end of systole (~380 ms after the ECG R wave). This wave is generated by the heart as a result of the decrease in the rate of myocardial shortening below the rate at which blood is flowing from the heart under its own momentum (24). This wave decelerates flow and contributes to aortic valve closure, and this wave may provide information regarding late-systolic or early-diastolic function (30). Interestingly, despite the marked increase in reflection from the body, AI_x was not significantly

increased in heart failure. AI_x is widely used as a surrogate measure of wave reflection but can be difficult to interpret since it is a composite of all reflections, and an identification of the point of inflection and magnitude of augmentation is influenced by the timing of reflections. Previous studies have yielded conflicting information regarding wave reflection and hemodynamics in heart failure. Two studies (17, 25) have reported impedance changes suggestive of increased wave reflections, but two others (13, 15) found no evidence of increased wave reflection. A more recent study (18) reported that wave reflection estimated by AI_x was actually decreased in heart failure. Wave intensity analysis gives a robust measure of wave reflection, and our study provides clear evidence for increased magnitude of wave reflection in heart failure without evidence that there is a change in timing in respect to the S wave.

Previous studies of arterial properties in heart failure are also inconsistent. Characteristic impedance of the aorta has been reported to be increased in some studies (18, 25) but not others (15, 17, 18). Carotid-femoral pulse wave velocity has been reported to be unchanged, whereas carotid-radial pulse wave velocity was reduced in the same study (18). Brachial artery compliance has been reported to be increased (19), unchanged (7), or decreased in heart failure (1). We found no increase in carotid artery wave speed, a measure of arterial stiffness, and no evidence that the timing of reflected waves was altered in heart failure. No waves were seen to appear in diastole in either normal individuals or subjects with heart failure, and these observations do not support the idea that the movement of a reflected wave from diastole to systole occurs in heart failure.

Our study has a number of limitations: measurements of pressure and flow velocity are measured sequentially as opposed to simultaneously, and, therefore, it was not possible to derive beat-by-beat wave intensities. In addition, the technique makes measurements in common carotid artery, and, although pressure waveforms in the carotid and the aorta are similar (3, 8), flow velocities waveforms differ in the common carotid artery and aorta, and, consequently, wave patterns may not be identical. Nevertheless, the patterns of wave intensity found in the carotid artery of normal subjects are similar to those found in the aorta of normal subjects and animals by previous investigators using invasive techniques (6, 12, 16, 32), suggesting that this is not a major limitation.

In summary, wave intensity analysis is an easily applicable tool that offers unique insights into cardiovascular pathophysiology. We have shown from noninvasive measurements of pressure and velocity in the common carotid artery that wave generation by the left ventricle is markedly impaired in heart failure and that wave reflection is increased, although wave speed and timing of arrival of the reflected wave with respect to the S wave are unaltered. Increased wave reflection in heart failure may add to the hemodynamic load experienced by the failing heart, and it is possible that therapeutic strategies aimed at reducing wave reflection may be useful in this condition.

ACKNOWLEDGMENTS

We are grateful to Dr D. Francis for helpful comments on the manuscript.

GRANTS

S. L. Curtis was supported in part by a grant from Astra-Zeneca.

REFERENCES

1. **Arnold JM, Marchiori GE, Imrie JR, Burton GL, Pflugfelder PW, Kostuk WJ.** Large artery function in patients with chronic heart failure. Studies of brachial artery diameter and hemodynamics. *Circulation* 84: 2418–2425, 1991.
2. **Braunwald E, Zipes DP, Libby P, Bonow R, eds.** *Braunwald's Heart Disease: A Textbook of Cardiovascular Medicine* (7th ed.). Philadephia, PA: Saunders, 2004.
3. **Chen CH, Nevo E, Fetics B, Pak PH, Yin FC, Maughan WL, Kass DA.** Estimation of central aortic pressure waveform by mathematical transformation of radical tonometry pressure—validation of generalized transfer function. *Circulation* 95: 1827–1836, 1997.
4. **Finkelstein SM, Cohn JN, Collins VR, Carlyle PF, Shelley WJ.** Vascular hemodynamic impedance in congestive heart failure. *Am J Cardiol* 55: 423–427, 1985.
5. **Hoskins PR.** Accuracy of maximum velocity estimates made using Doppler ultrasound systems. *Br J Radiol* 69: 172–177, 1996.
6. **Jones CJ, Sugawara M.** "Wavefronts" in the aorta—implications for the mechanisms of left ventricular ejection and aortic valve closure. *Cardiovasc Res* 27: 1902–1905, 1993.
7. **Kaiser DR, Mullen K, Bank AJ.** Brachial artery elastic mechanics in patients with heart failure. *Hypertension* 38: 1440–1445, 2001.
8. **Karamanoglu M, Feneley MP.** Derivation of the ascending aortic-carotid pressure transfer function with an arterial model. *Am J Physiol Heart Circ Physiol* 271: H2399–H2404, 1996.
9. **Kelly R, Fitchett D.** Noninvasive determination of aortic input impedance and external left ventricular power output: a validation and repeatability study of a new technique. *J Am Coll Cardiol* 20: 952–963, 1992.
10. **Kelly R, Hayward C, Avolio A, O'Rourke M.** Noninvasive determination of age-related changes in the human arterial pulse. *Circulation* 80: 1652–1659, 1989.
11. **Khir AW, O'Brien A, Gibbs JS, Parker KH.** Determination of wave speed and wave separation in the arteries. *J Biomech* 34: 1145–1155, 2001.
12. **Koh TW, Pepper JR, DeSouza AC, Parker KH.** Analysis of wave reflections in the arterial system using wave intensity: a novel method for predicting the timing and amplitude of reflected waves. *Heart Vessels* 13: 103–113, 1998.
13. **Kromer EP, Elsner D, Holmer SR, Muntze A, Riegger GA.** Aortic input impedence and neurohormonal activation in patients with mild to moderate chronic congestive heart failure. *Cardiovasc Res* 26: 265–272, 1992.
14. **Kromer EP, Riegger GA.** Aortic input impedance in mild to moderate chronic congestive heart failure: lack of interrelation with neurohormonal activation. *Eur Heart J* 13, *Suppl* E: 113–118, 1992.
15. **Laskey WK, Kussmaul WG.** Arterial wave reflection in heart failure. *Circulation* 75: 711–722, 1987.
16. **MacRae JM, Sun YH, Isaac DL, Dobson GM, Cheng CP, Little WC, Parker KH, Tyberg JV.** Wave-intensity analysis: a new approach to left ventricular filling dynamics. *Heart Vessels* 12: 53–59, 1997.
17. **Merillon JP, Fontenier G, Lerallut JF, Jaffrin MY, Chastre J, Assayag P, Motte G, Gourgon R.** Aortic input impedance in heart failure: comparison with normal subjects and its changes during vasodilator therapy. *Eur Heart J* 5: 447–455, 1984.
18. **Mitchell GF, Tardif JC, Arnold JM, Marchiori G, O'Brien TX, Dunlap ME, Pfeffer MA.** Pulsatile hemodynamics in congestive heart failure. *Hypertension* 38: 1433–1439, 2001.
19. **Nakamura M, Sugawara S, Arakawa N, Nagano M, Shizuka T, Shimoda Y, Sakai T, Hiramori K.** Reduced vascular compliance is associated with impaired endothelium-dependent dilatation in the brachial artery of patients with congestive heart failure. *J Card Fail* 10: 36–42, 2004.
20. **Nichols WV, O'Rourke MF.** *McDonald's blood flow in arteries. Theoretical, Experimental and Clinical Principles*. London: Edward Arnold, 1998.
21. **Nichols WW, Estrada JC, Braith RW, Owens K, Conti CR.** Enhanced external counterpulsation treatment improves arterial wall properties and wave reflection characteristics in patients with refractory angina. *J Am Coll Cardiol* 48: 1208–1214, 2006.
22. **Niki K, Sugawara M, Uchida K, Tanaka R, Tanimoto K, Imamura H, Sakomura Y, Ishizuka N, Koyanagi H, Kasanuki H.** A noninvasive method of measuring wave intensity, a new hemodynamic index: application to the carotid artery in patients with mitral regurgitation before and after surgery. *Heart Vessels* 14: 263–271, 1999.

23. **Parker KH, Jones CJ.** Forward and backward running waves in the arteries: analysis using the method of characteristics. *J Biomech Eng* 112: 322–326, 1990.
24. **Parker KH, Jones CJ, Dawson JR, Gibson DG.** What stops the flow of blood from the heart? *Heart Vessels* 4: 241–245, 1988.
25. **Pepine CJ, Nichols WW, Conti CR.** Aortic input impedance in heart failure. *Circulation* 58: 460–465, 1978.
26. **Ramsey MW, Goodfellow J, Jones CJ, Luddington LA, Lewis MJ, Henderson AH.** Endothelial control of arterial distensibility is impaired in chronic heart failure. *Circulation* 92: 3212–3219, 1995.
27. **Schiller NB, Shah PM, Crawford M, DeMaria A, Devereux R, Feigenbaum H, Gutgesell H, Reichek N, Sahn D, Schnittger I, Silverman NH, Tajik AJ.** Recommendations for quantification of the left ventricle by two-dimensional echcardiography. American Society of Echocardiography Committee on Standards, Subcommittee on Quantitation of Two-Dimensional Echcardiograms. *J Am Soc Echocardiogr* 2: 358–367, 1989.
28. **Stein PD, Blick EF.** Arterial tonometry for the atraumatic measurement of arterial blood pressure. *J Appl Physiol* 30: 593–596, 1971.
29. **Suga H.** Global cardiac function: mechano-energetico-informatics. *J Biomech* 36: 713–720, 2003.
30. **Sugawara M, Uchida K, Kondoh Y, Magosaki N, Niki K, Jones CJ, Sugimachi M, Sunagawa K.** Aortic blood momentum—the more the better for the ejecting heart in vivo? *Cardiovasc Res* 33: 433–446, 1997.
31. **Van Bortel LM, Balkestein EJ, van der Heijden-Spek JJ, Vanmolkot FH, Staessen JA, Kragten JA, Vredeveld JW, Safar ME, Struijker Boudier HA, Hoeks AP.** Non-invasive assessment of local arterial pulse pressure: comparison of applanation tonometry and echo-tracking. *J Hypertens* 19: 1037–1044, 2001.
32. **Zambanini A, Cunningham SL, Parker KH, Khir AW, McG Thom SA, Hughes AD.** Wave-energy patterns in carotid, brachial, and radial arteries: a noninvasive approach using wave-intensity analysis. *Am J Physiol Heart Circ Physiol* 289: H270–H276, 2005.
33. **Zambanini A, Khir AW, Byrd SM, Parker KH, McG Thom SA, Hughes AD.** Wave intensity analysis: a novel non-invasive method for determining arterial wave transmission. *Comput Cardiol* 29: 717–720, 2002.